

## Betaine arsenate as a system with two instabilities

E. V. Balashova, V. V. Lemanov, A. K. Tagantsev,\* A. B. Sherman, and Sh. H. Shomuradov  
*A. F. Ioffe Physico-Technical Institute of Russian Academy of Sciences, 194021 St. Petersburg, Russia*  
 (Received 5 July 1994)

Using our experimental dielectric and acoustic data and those available in the literature (the small-signal dielectric response, the temperature evolution of the dielectric hysteresis loops, the electric-field-temperature phase diagram, the sequence and the types of the observed phase transitions, the temperature-deuterium-concentration phase diagram and partial temperature loops in the sound velocity), we analyze the properties of a  $(\text{CH}_3)_2\text{NCH}_2\text{COO}\cdot\text{H}_3\text{AsO}_4$ - $(\text{CH}_3)_2\text{NCH}_2\text{COO}\cdot\text{D}_3\text{AsO}_4$  solid solution in the framework of a unique phenomenological scheme corresponding to a system with two competing instabilities (ferroelectric and structural). We average the competition on a macroscopical level, where the coexistence of the two types of ordering is, in principle, possible, but the appearance of one of the order parameters suppresses the instability related to the other. It is shown that betaine arsenate-deuterated betaine arsenate represents a good example of such a system.

### I. INTRODUCTION

The study of a system with competing interactions has been under intensive consideration for many years.<sup>1</sup> Normally, when discussing this problem, one averages competition on a microscopic level, i.e. a ferromagnetic interaction between nearest neighbors and an antiferromagnetic one between next-nearest neighbors. This type of interaction often results in an incommensurate phase or series of many phase transitions close in the temperature. However, one can find another type of competing interaction on the macroscopic level, i.e., the situation where the coexistence of the two types of ordering is, in principle, possible, but the appearance of one of the order parameters suppresses the instability related to the other. In this case we are mainly dealing with a competition between several homogeneous ordered phases, having an inhomogeneous phase only in a very narrow interval of the model parameters. Systems of this type have been theoretically studied comprehensively,<sup>2-4</sup> manifesting a set of interesting properties, however, to the best of our knowledge, this set has never been demonstrated in the same material. In this paper we shall try to do that.

Solid solutions of betaine arsenate  $(\text{CH}_3)_2\text{NCH}_2\text{COO}\cdot\text{H}_3\text{AsO}_4$  (BA) and deuterated betaine arsenate  $(\text{CH}_3)_2\text{NCH}_2\text{COO}\cdot\text{D}_3\text{AsO}_4$  (DBA) are a very interesting system with ferroelectric and antiferroelectric properties.<sup>5</sup> BA and DBA undergo a ferroelastic phase transition ( $Pcnm$ - $P12_1/n$ ) at  $T_{c1}=411$  K. At lower temperatures BA transforms into a ferroelectric state ( $P12_1/n$ - $Pn$ ) at  $T_{c2}=119$  K and DBA transforms into an antiferroelectric state at  $T_{c2}=172$  K.<sup>5-7</sup> At first the ferroelectric phase transition temperature increases with the increasing of the deuteration degree. But when the degree of deuteration exceeds 80%, the ferroelectric phase transition line splits into antiferroelectric ( $T_{c2}$ ) and ferroelectric ( $T_{c3}$ ) branches (Fig. 1).<sup>6,7</sup> As a result in high deuterated betaine arsenate there occurs the sequence of second-order antiferroelectric and first-order ferroelectric

phase transitions.

We believe that BA-DBA solid solution represents a good example of a system with two competing instabilities (ferroelectric and structural). We shall try to demonstrate this example using our experimental dielectric and acoustic data, existing experimental data, and the results of the phenomenological analysis of the two-instability system.<sup>4</sup> We shall show that many properties of BA-DBA (the small-signal dielectric response, the temperature evolution of the hysteresis loops, the temperature-electric-field phase diagram, the sequence and the types of the observed phase transitions, and the temperature-deuterium-concentration phase diagram) can be interpreted in the framework of one phenomenological scheme and that in some cases a quantitative agreement between the properties can be demonstrated.

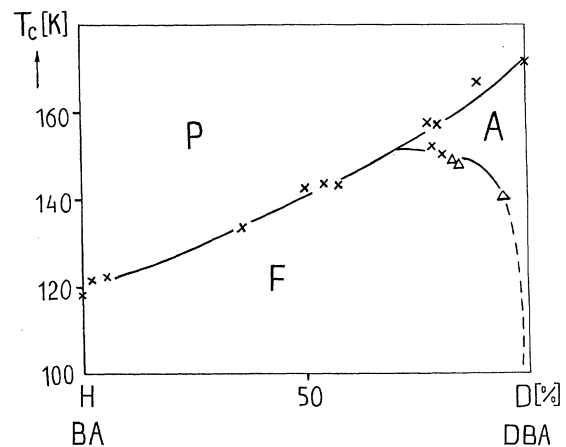


FIG. 1. Phase diagram for BA-DBA system (Refs. 6 and 7). P, paraelectric phase; F, ferroelectric phase; A, antiferroelectric phase.

## II. EXPERIMENTAL RESULTS

Dielectric and acoustic properties of DBA crystals with deuterium concentration 85% (DBA85) and 90% (DBA90) have been studied. For dielectric measurements thermally evaporated Cr electrodes have been used. Acoustic measurements have been performed by the echo-pulse method with an accuracy of  $10^{-4}$  for velocity.

Since, in the ferroelectric phase, polarization  $P_z$  is about ten times larger than  $P_x$ , we paid the main attention to the  $\epsilon_{zz}$  component of the dielectric constant. The temperature dependences of the dielectric constant  $\epsilon_{zz}$  and reciprocal dielectric constant of DBA85 at the frequency 1 kHz are shown in Figs. 2(a) and 2(b). Two maximums of  $\epsilon_{zz}$  for the antiferroelectric and ferroelectric phase transition are observed. It is worth noting that the large maximum of  $\epsilon_{zz}$  corresponds to the antiferroelectric phase transition and the rather small maximum to the ferroelectric phase transition at  $T_{c3}$ .

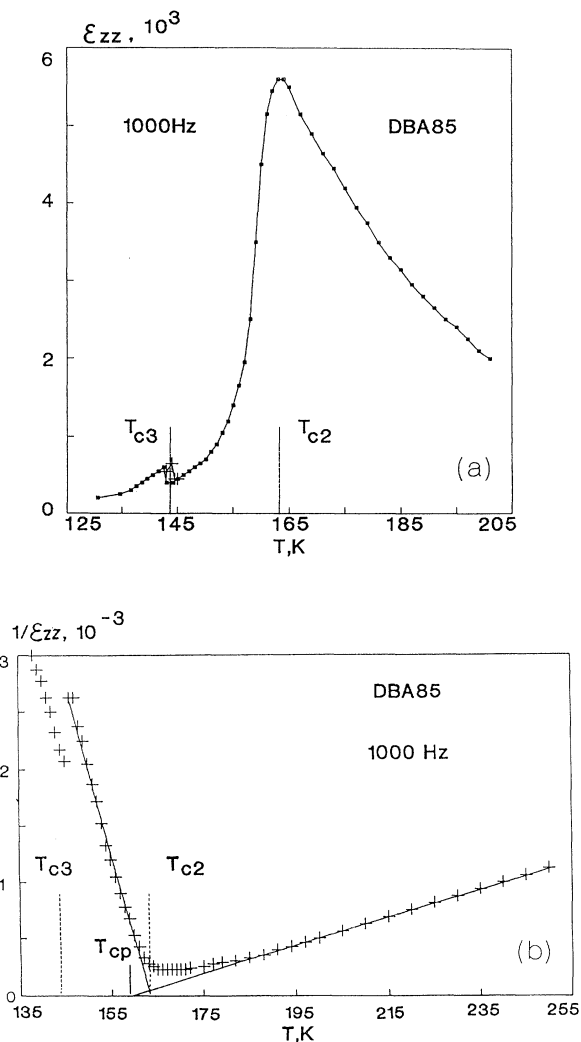


FIG. 2. Temperature dependences of dielectric constant  $\epsilon_{zz}$  (a) and reciprocal dielectric constant  $1/\epsilon_{zz}$  (b).

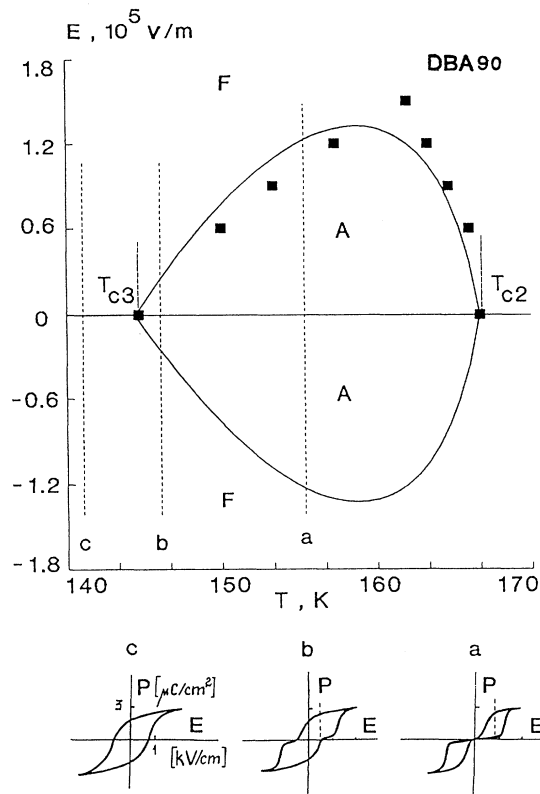


FIG. 3.  $E$ - $T$  phase diagram ( $\square$ , experiment; —, calculation) and dielectric hysteresis loop (corresponding to cross sections  $a$ ,  $b$ , and  $c$ ) at frequency 50 Hz in DBA90.

Figure 3 shows the experimental  $E$ - $T$  phase diagram for DBA90 which was deduced from measurements of the temperature dependence of the dielectric constant in the presence of bias electric fields. We observed the considerable shift of the ferroelectric phase transition point to higher temperatures under the action of the bias fields. At bias fields of more than  $1.3 \times 10^5$  V/m the intermediate antiferroelectric state disappears. This  $E$ - $T$  phase diagram corresponds to the convergence of the double hysteresis loop and its conversion into the single loop with decreasing temperature, which we observed in our experiment and which also was reported earlier in Ref. 6.

In Fig. 4(a), the temperature dependence of the velocity of longitudinal acoustic waves at the frequency 15 MHz propagating along the  $Z$  axis in DBA85 is shown. One can see also two anomalies related to the antiferroelectric and ferroelectric phase transitions.<sup>8</sup> It should be noted that along with the positive jumps of the velocity at the first-order ferroelectric phase transition ( $T_{c3}$ ) with the hysteresis about 2 K we observed the temperature hysteresis of velocity in a larger temperature range.

The partial temperature hysteresis loops in the velocity have been studied for the ferroelectric phase of DBA85. One of the partial temperature loops is shown in Fig. 4(b). This loop has such a specific feature, which is often observed in crystals with incommensurate structures.<sup>9</sup>

### III. DISCUSSION

Analysis of the experimental results shows that the BA-DBA system belongs to the "S region" as follows from the two-order-parameter phenomenological model developed in Ref. 4. In Ref. 4, the dielectric behavior of the system with ferroelectric and structural instabilities was studied in the framework of the following Landau free energy expansion:

$$F = \frac{1}{2}\alpha_1\eta^2 + \frac{1}{4}\beta_1\eta^4 + \frac{1}{2}\alpha_2P^2 + \frac{1}{4}\beta_2P^4 + \frac{1}{2}\gamma\eta^2P^2 - PE, \quad (1)$$

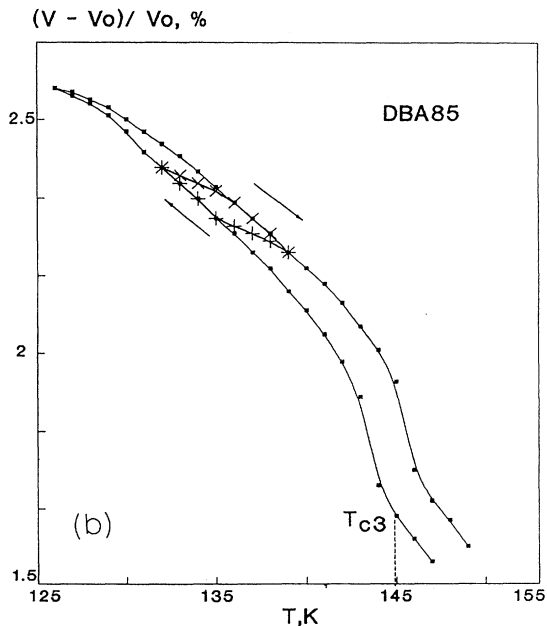
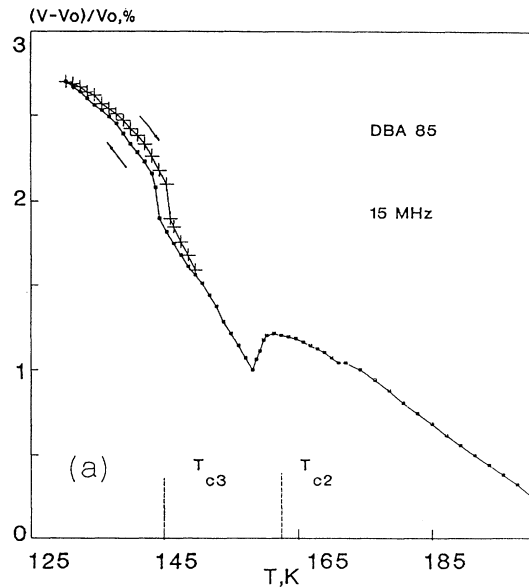


FIG. 4. Temperature dependences of velocity of longitudinal acoustic wave in  $Z$  direction (a) and partial temperature hysteresis loop in velocity (b).

where  $\eta$  is a structural order parameter,  $P$  is the polarization,  $E$  is the macroscopic electric field parallel to the polar axis,  $\alpha_1 = \lambda_1(T - T_{c\eta})$ ,  $\alpha_2 = \lambda_2(T - T_{cP})$ , and  $\beta_1$ ,  $\beta_2$ , and  $\gamma$  are positive. We identify  $T_{c\eta}$  with the antiferroelectric transition temperature  $T_{c2}$ .

Using dielectric data, such as the small-signal response, the response to strong electric fields (hysteresis phenomena included), and the phase diagram in the presence of the bias field, one can single out six qualitatively different types of behavior of the model. Only two independent parameters  $\Delta$  and  $\varphi$  govern the separation:

$$\Delta = (\lambda_1/\lambda_2)(\beta_2/\beta_1)^{1/2} \quad \text{and} \quad \varphi = \gamma(\beta_1\beta_2)^{-1/2}. \quad (2)$$

The parameter  $\Delta$  reflects the difference in the temperature dependences between the energies for the nonpolar ordered state ( $P=0, \eta \neq 0$ ) and polar state ( $P \neq 0, \eta=0$ ); the parameter  $\varphi$  determines the coupling between the order parameters.

There are several regions in the  $(\Delta, \varphi)$  plane, which correspond to the different dielectric behavior (Fig. 5). The BA-DBA system is ascribed to the  $S$  region. This region is the most interesting among all six regions because it can be considered as an intermediate one between the "classic" antiferroelectric behavior ( $U, T$  regions) and the ferroelectric behavior ( $W1, W2, I$  regions). The systems which belong to the  $S$  region manifest the sequence of the antiferroelectric and noncritical first-order ferroelectric phase transitions, the latter being accompanied by a weak dielectric anomaly.<sup>4</sup> These systems also manifest the double "antiferroelectric" hysteresis loops converging on cooling and converting finally into a single "ferroelectric" hysteresis loop.

For the  $S$  region, two conditions for the independent parameters are valid:  $\varphi\Delta > 1$  and  $\Delta < 1$ . The first condition means that the structural order parameter, which appears at  $T < T_{c\eta}$ , suppresses completely the ferroelectric instability, i.e., the critical ferroelectric phase transition is impossible because in the temperature range below  $T_{c\eta}$  there is no point where the nonpolar ordered state with  $\eta \neq 0$  loses its stability. The second condition ( $\Delta < 1$ ) means that the energy of the polar state changes with temperature faster than that of the nonpolar ordered

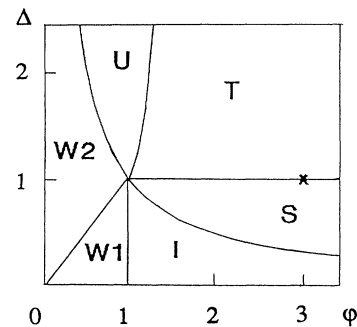


FIG. 5. The classification of different types of dielectric behavior in the  $(\varphi, \Delta)$  plane from Ref. 4. The cross shows the values of the parameters ( $\Delta=1$  and  $\varphi=3$ ) at which the considered model is equivalent to the Kittel model.

state. Temperature dependences of the energy of the states are schematically shown in Fig. 6(a). In this case, there is a temperature ( $T_c$ ) where the energies of the two states are equal and therefore, for  $T < T_c$ , the aforementioned polar phase appears by means of the noncritical first-order ferroelectric phase transition.

The reasons for referring the BA-DBA system to the  $S$  region are the following: (i) the type of  $\varepsilon_{zz}$  temperature dependence; (ii) the “antiferroelectric” hysteresis loops which converge on cooling and finally transform into a single “ferroelectric” loop; (iii) the  $E$ - $T$  phase diagram. These three facts can be considered as a qualitative identification of the system. However, one can perform this identification quantitatively, namely, one can calculate  $\Delta$  and  $\varphi$  from one set of properties, then verify that the values found belong to the  $S$  region of the diagram and, finally, using these values, determine parameters related to other properties and compare the result of the calculation to the experimental data. We shall perform this process using the small-signal dielectric response as an initial set of properties and the  $E$ - $T$  and deuteration phase diagrams as verification.

Using the data of the temperature dependences of  $\varepsilon_{zz}$  and  $1/\varepsilon_{zz}$  shown in Fig. 2 and Eq. (A3) and (A8) derived in the Appendix, we calculate the  $\Delta$  and  $\varphi$  parameters. These equations are

$$T_c = (T_{cp} - \Delta T_{c\eta}) / (1 - \Delta), \quad (3)$$

$$b/a = 1 - \varphi\Delta, \quad (4)$$

where  $a$  and  $b$  are the slopes of the reciprocal dielectric constant (plotted against the temperature) in the paraelectric and nonpolar ordered states, respectively.  $T_{c\eta} = T_{c2} = 162.5$  K is the structural (antiferroelectric) phase transition point and  $T_{cp} = 158$  K is the temperature, where the reciprocal dielectric constant extrapolated by the Curie-Weiss law from the paraelectric phase becomes zero. We identify  $T_c$  with  $T_{c3} = 144$  K. From Eqs. (3) and (4) we find  $\varphi = 15$ ,  $\Delta = 0.76$  for DBA85. Performing the same calculation for DBA90 we find  $\varphi = 15$  and  $\Delta = 0.78$ . Thus,  $\varphi$  does not depend on the degree of deuteration and  $\Delta$  has a weak dependence. Now, knowing the values of the parameters we can calculate the  $E$ - $T$  phase diagram, using the theoretical results.<sup>4</sup> The calcu-

lated phase diagram is shown in Fig. 3 as a solid line. The calculated curve is in good agreement with the experimental data.

The  $E$ - $T$  phase diagram allows us to explain the temperature behavior of the dielectric hysteresis loop. The boundary between the antiferroelectric state, where  $\eta \neq 0$ , and the ferroelectric state, where  $\eta = 0$ , is the line of the bias-field-induced phase transition. This transition can be of first or second order. Using the results of Ref. 4 [see Eq. (A9) in the Appendix] one finds the temperature  $T_b$

$$T_b = T_{c\eta} - \frac{\varphi(T_{c\eta} - T_{cp})}{\varphi(1 - \varphi\Delta) + 3\Delta(\varphi^2 - 1)} \quad (5)$$

separating the region of the second-order phase transition ( $T_b < T < T_{c2}$ ) from that of the first order ( $T_{c3} < T < T_b$ ). Using the parameters of the model determined for DBA90 ( $\Delta = 0.78$ ,  $\varphi = 15$ ,  $T_{c\eta} = 167$  K,  $T_{cp} = 162$  K) one finds  $T_b = T_{c\eta} - 0.11$  K. Thus, almost in the whole temperature interval  $T_{c3} < T < T_{c2}$  the boundary between states corresponds to the first-order phase transition under an external electric field.

In this case, the double dielectric hysteresis loops should be observed when crossing the border line between two phases. When approaching the  $T_{c3}$  point from above, the value of electric field, which is necessary to switch one state into the other, decreases. It means that the double hysteresis loops converge on cooling and finally continuously transform into a single ferroelectric loop below  $T_{c3}$ . Just this temperature behavior of hysteresis loop has been observed in DBA.

Thus, we have shown that DBA crystals are a system with two coupled polar and structural instabilities. From this point of view we can now describe the phase diagram of the BA-DBA system, shown in Fig. 1. Analyzing this phase diagram we see that the polar instability manifests itself in the critical ferroelectric phase transition at the deuterium concentration from 0 to 80%. At the same time, the structural instability manifests itself in the antiferroelectric phase transition at the deuterium concentration from 80% to 100%. It is worth noting that each instability has a different slope of phase transition point versus deuterium concentrations  $D$ :  $\partial T_{cp} / \partial D < \partial T_{c\eta} / \partial D$ . Using a linear approximation for these experimental dependences, the resulting phase diagram is shown in Fig. 7, where broken lines are the extension of the lines of the ferroelectric and antiferroelectric instabilities into the concentration region where these instabilities are not realized in a critical phase transition. When deuteration degree exceeds 80% the structural instability is realized before the ferroelectric one at temperature  $T_{c\eta} > T_{cp}$  and the polar state appears by means of a noncritical first-order phase transition at  $T_c$ . This transition is a result of the different temperature dependence of the energies of the polar and nonpolar ordered states as shown in Fig. 6(a). At low deuterium concentration, we have another situation. In this case  $T_{cp} > T_{c\eta}$ , the structural instability is suppressed by the polar order parameter and the nonpolar ordered state does not arise at all. That is due to the fact that, in this case, the energy of the ferroelectric state ( $P \neq 0$ ,  $\eta = 0$ ) is lower than that of

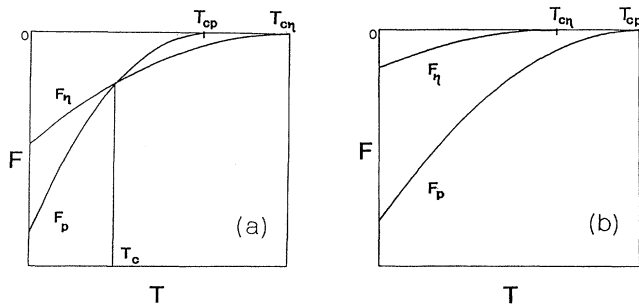


FIG. 6. Schematic temperature dependences of the energies of polar  $F_p$  and nonpolar  $F_\eta$  ordered states: (a)  $T_{c\eta} > T_{cp}$ ; (b)  $T_{c\eta} < T_{cp}$ .

the nonpolar state ( $P=0$ ,  $\eta \neq 0$ ) at any temperature [Fig. 6(b)].

We have explained the phase diagram of the BA-DBA system qualitatively. We can describe it quantitatively too, using the theory developed in Ref. 4. One can see from Eq. (3) that there exists a relation between  $T_{c\eta}$ ,  $T_{cp}$ ,  $T_c$ , and  $\Delta$ . From experimental data shown in Figs. 1 and 7, we can calculate the slopes of the phase transition lines:  $\partial T_{c\eta}/\partial D = 0.75$  and  $\partial T_{cp}/\partial D = 0.45$  (K/%). From Eq. (3) we get the expression for the slope of the noncritical first-order ferroelectric phase transition line:

$$\frac{\partial T_c}{\partial D} = \frac{\partial T_{cp}/\partial D - \Delta \partial T_{c\eta}/\partial D}{1 - \Delta} \quad (6)$$

(we neglect a weak concentration dependence of  $\Delta$ ). Finally, taking  $\Delta = 0.76$  we find  $\partial T_c/\partial D = -0.5$  (K/%), that is in good agreement with the experimental data.

One of the interesting properties of the BA-DBA system is the specific hysteresis phenomena observed in the acoustic properties. The shape of the temperature hysteresis loops is quite similar to that observed in incommensurate phases.<sup>9</sup> We believe that this behavior indeed attests to the existence of an incommensurate phase in our crystal. The arguments in favor of the incommensurate phase are as follows. The symmetry of the paraelectric phase is sufficiently low ( $P12_1/n$ ) to permit the nonlinear Lifshitz invariants in the free energy expansion:

$$\begin{aligned} \eta^2(\partial P_x/\partial z) - P_x(\partial \eta^2/\partial z), \\ \eta^2(\partial P_z/\partial x) - P_z(\partial \eta^2/\partial x) \end{aligned} \quad (7)$$

If we suppose that the order parameter  $\eta$  transforms according to the unity representation then the linear Lifshitz invariants are possible too:

$$\begin{aligned} \eta(\partial P_x/\partial z) - P_x(\partial \eta/\partial z), \\ \eta(\partial P_z/\partial x) - P_z(\partial \eta/\partial x). \end{aligned} \quad (8)$$

Any of the four aforementioned invariants Eqs. (7) and

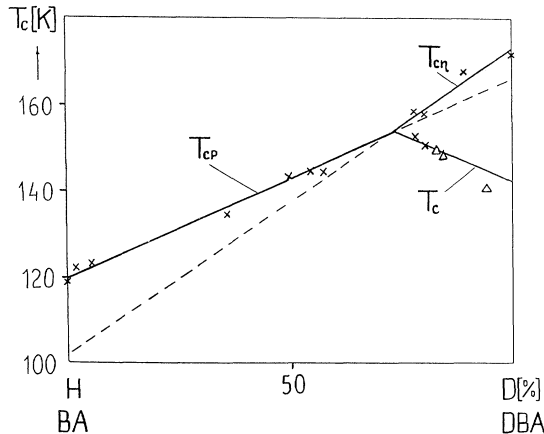


FIG. 7. Linear approximation of the phase diagram for the BA-DBA system, shown in Fig. 1. The  $T_{cp}$  and  $T_{c\eta}$  lines are linear approximations of the experimental curves. The  $T_c$  line is calculated using Eq. (6).

(8) leads inevitably to the appearance of an incommensurate phase if the instability temperatures  $T_{c\eta}$  and  $T_{cp}$  are close enough. The case related to the invariants Eq. (8) has been investigated in detail by Golovko<sup>2</sup> and the case related to Eq. (7) has been studied by Korzhenevskii.<sup>3</sup>

We believe that an incommensurate phase of the type discussed in Refs. 2 and 3 is observed in our experiment, manifesting itself in specific temperature hysteresis loops in sound velocity. However, the lack of information on the symmetry of the nonpolar order parameter  $\eta$  prevents a decision on which invariant [Eq. (7) or Eq. (8)] is responsible for the appearance of the incommensurate phase.

#### IV. CONCLUSIONS

Dielectric and acoustic properties of the BA-DBA system have been studied. Using these data and those available in the literature, we have analyzed the behavior of this material in terms of a system with two competing instabilities. It was shown that, exhibiting many characteristic properties of the two-instability system, BA-DBA can be considered as a classical example of a system of this type.

#### ACKNOWLEDGMENTS

All the authors are indebted to Dr. J. Albers for crystal growth. E.V.B., A.K.T., and A.B.S. gratefully acknowledge the American Physical Society for a Soros Foundation Grant. A.E. Glazunov is acknowledged for a critical reading of the manuscript.

#### APPENDIX

In Ref. 4 the noncritical ferroelectric phase transition temperature was found in dimensionless units:

$$t_c = -(1 - \Delta)^{-1}, \quad (A1)$$

where

$$t_c = \frac{T_c - T_{c\eta}}{T_{c\eta} - T_{cp}}. \quad (A2)$$

Using (A1) and (A2) we get the equation for  $T_c$  in the explicit form

$$T_{cp} = \frac{T_{c\eta} - \Delta T_c}{1 - \Delta}. \quad (A3)$$

From Ref. 4 the equations for the reciprocal dielectric susceptibility in dimensionless units in the paraelectric and nonpolar ordered states, respectively, are

$$X^{-1} = 1 + t, \quad (A4)$$

$$X^{-1} = 1 + t(1 - \varphi\Delta). \quad (A5)$$

From Eqs. (A4) and (A5) one can determine the slopes of temperature dependences of the reciprocal dielectric susceptibility in both phases, respectively:

$$a = \frac{\partial X^{-1}}{\partial t} = 1, \quad (A6)$$

$$b = \frac{\partial X^{-1}}{\partial t} = 1 - \varphi\Delta. \quad (A7)$$

The ratio of the slopes is

$$b/a = 1 - \varphi\Delta . \quad (\text{A8})$$

From Ref. 4 the criterion for the first-order phase transition is

$$t < t_b = - \frac{\varphi}{\varphi(1 - \varphi\Delta) + 3\Delta(\varphi^2 - 1)} , \quad (\text{A9})$$

where  $t$  is the temperature in dimensionless units:

$$t = \frac{T - T_{c\eta}}{T_{c\eta} - T_{cp}} . \quad (\text{A10})$$

\*Also at Laboratoire de Céramique, Département des Matériaux, École Polytechnique Fédérale de Lausanne, Lausanne CH 1015, Switzerland.

<sup>1</sup>R. S. Gekht and V. I. Ponomarev, *Phase Trans.* **20**, (1990).

<sup>2</sup>V. A. Golovko, *Fiz. Tverd. Tela* **22**, 2960 (1980) [*Sov. Phys. Solid State* **22**, 1729 (1980)]; **25**, 2816 (1983) [**25**, 1625 (1983)].

<sup>3</sup>A. L. Korzhenevskii, *Zh. Eksp. Teor. Fiz.* **81**, 1071 (1981) [*Sov. Phys. JETP* **54**, 568 (1981)]; *Pis'ma Zh. Eksp. Teor. Fiz.* **35**, 315 (1982) [*JETP Lett.* **35**, 386 (1982)].

<sup>4</sup>E. V. Balashova and A. K. Tagantsev, *Phys. Rev. B* **48**, 9979

(1993).

<sup>5</sup>J. Albers, *Ferroelectrics* **79**, 3 (1988).

<sup>6</sup>H. J. Rother, J. Albers, A. Klöpperpieper, and H. E. Müser, *Jpn. J. Appl. Phys., Suppl.* **24-2**, 384 (1985).

<sup>7</sup>G. Schaak, *Ferroelectrics* **104**, 147 (1990).

<sup>8</sup>J. Albers, E. V. Balashova, A. Klöpperpieper, V. V. Lemanov, H. E. Müser, and A. b. Sherman, *Ferroelectrics* **125**, 315 (1992).

<sup>9</sup>B. A. Strukov, N. Uesu, and V. M. Aruyunova, *Pis'ma Zh. Eksp. Teor. Fiz.* **35**, 524 (1982) [*JETP Lett.* **35**, 424 (1982)].